

# Crosswind Effects on the Stability of High-Speed Trains

Eyad Ayman Hany, Hamdy Gamal Rashad, Amr Shrief AbdelHafeez, Mohamed Ahmed Abdel Azeez, Mohamed Ahmed Abdel Fatah Akl, Mohamed Hassan Mohamed Hassan, Mohamed Hany Metwaly Zaki  
Mechanical Power Engineering Dept., Faculty of Engineering, Zagazig University, Egypt, [eyadayman9922@gmail.com](mailto:eyadayman9922@gmail.com),

[hamdysheref9@gmail.com](mailto:hamdysheref9@gmail.com), [amrshrief00@gmail.com](mailto:amrshrief00@gmail.com), [mo\\_ahmed99@gmail.com](mailto:mo_ahmed99@gmail.com), [muhma03@gmail.com](mailto:muhma03@gmail.com),

[m01098948741@gmail.com](mailto:m01098948741@gmail.com), [mohamezhanz12345@gmail.com](mailto:mohamezhanz12345@gmail.com).

Supervisors:

Prof. Dr. Ahmed Farouk AbdelGawad

Prof. Dr. Mofreh Melad Nassief

Faculty of Engineering, Zagazig University, Egypt, [afaroukgb@gmail.com](mailto:afaroukgb@gmail.com), [mofreh\\_melad@yahoo.com](mailto:mofreh_melad@yahoo.com).

**Abstract**– This paper gives details of the simulation model including method, flow field, corresponding boundary conditions, geometry, and computational mesh. It then shows the train's aerodynamic flow and loads with a range of variable operating speeds and incoming wind speeds. The aerodynamic interaction between a moving train and the transverse wind is expressed in terms of the flow features around the train, variable yaw angles, and the effect of the moving train on the aerodynamic forces of the train including lateral force, lift force, and rolling moment. This work contains different cases for three basic factors, namely: wind speed, train speed, and yaw angle. Firstly, the train speed is 100 km/h, with a wind speed of 12 m/s, and wind angles of 0, 30, 60, and 90 degrees. Secondly, the train speed is 300 km/h, with a wind speed of 15 m/s, and wind angles of 0, 30, 60, and 90 degrees. Good results and important conclusions are recorded.

**Keywords**-- CFD, Train, Stability Crosswind, Overturning

## I. INTRODUCTION

High-speed rail is a general trend in the development of global rail transport, and it is also a key indicator of railway technology modernization. In recent years, high-speed rail has gained worldwide attention and rapid development.[1]

With increasing train speed, the interaction between the high-speed train and the surrounding air becomes more and more obvious, and the dynamic environment of the train changes from mechanical superiority to aerodynamic advantage. Aerodynamics has become a key technological challenge for high-speed trains.

When high-speed trains near the ground in the atmosphere reach speeds of 205-300 km/h, the drag of the train comes primarily from the surrounding air, and air resistance can account for 75% of the total drag. Aerodynamic resistance is proportional to the second order of train speed and becomes a large percentage of the total drag as train speed increases. Air resistance is becoming one of the main factors limiting train speed and saving energy.[1]

Drag reduction plays a very important role in the aerodynamic design of high-speed trains. In addition, other aerodynamic forces (moments) are also proportional to the

quadratic of equation of train speed. Aerodynamic force (moment) increases rapidly with the speed of the train and can reduce the operational safety of high-speed trains.

The flow field of high-speed trains changes drastically due to strong crosswinds, and aerodynamic lateral force, lift and rolling moment increase sharply, which have a great impact on train driving safety. When trains are traveling at high speeds in the atmosphere, the pressure on the train surface can change rapidly, especially in combination with oncoming trains and trains passing through tunnels.

Transient pressure pulses can have a significant impact on the strength of the car body and windows. In the aerodynamic design of high-speed trains, it is very important to reduce the pressure waves of passing trains and trains passing through tunnels and to improve the air-tightness strength. Aerodynamic noise is also an important issue caused by increasing train speeds. When the train speed reaches 300km/h, aerodynamic noise drowns out wheel-railroad noise. This is a major challenge to reduce aerodynamic noise from high-speed trains. Therefore, high-speed trains require aerodynamic design, which is rarely taken into account in traditional trains.

The presence of crosswinds and possible problems question the benefits of high-speed trains. The crosswind stability of high-speed trains needs to be studied carefully.

## II. DEFINITION OF FORCES

When trains are subject to a crosswind, they experience three aerodynamic forces (drag force  $F_d$ , side force  $F_s$  and lift force  $F_l$  along the x, y and z axes, respectively) and three aerodynamic moments (rolling moment  $M_{RL}$  about the x axis, pitching moment  $M_P$  about the y axis and yawing moment  $M_y$  about the z axis). [2]The origin for the coordinate system is usually taken to be at the center of the track at rail level, below the geometric longitudinal center of the vehicle being considered, Fig.1.

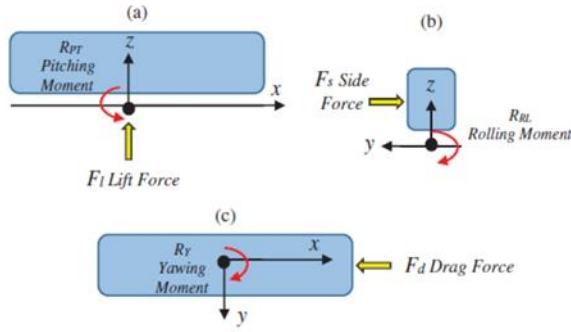


Fig. 1: Forces and moment, on train in three dimensions.[2]

### III. RESEARCH TOPICS RELATED TO TRAIN AERODYNAMICS

#### A. Aerodynamic Resistance

The coefficient for the aerodynamic drag is calculated as follows:

$$C_d = \frac{F_d}{0.5\rho v^2 A} \quad (1)$$

Where,  $F_d$  is the force in driving direction,  $\rho$  is the air density,  $V$  denotes the driving speed, and  $A$  represents the reference area, which is standardized to be 10 m<sup>2</sup> within the train aerodynamics community. [2]

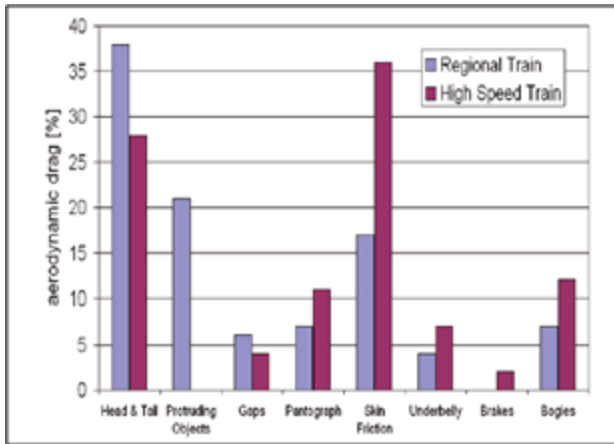


Fig. 2: Typical drag distribution for high-speed trains and regional trains.

Fig. 2 provides an overview of the specific contributions of the various components of a typical regional and high-speed train in the aerodynamic drag.[3]

There are three ways to reduce the aerodynamic drag of a high-speed train. First, is to optimize the design of the streamlined head. Second, is to design a smooth train body surface (smoothing the key parts of the train body, such as the pantograph, wheel truck, and windshield areas). Third, is to use flow control technology (bionic design or turbulence control).[3]

#### B. Safety issues with crosswind

6<sup>th</sup> IUGRC International Undergraduate Research Conference, Military Technical College, Cairo, Egypt, Sep. 5<sup>th</sup> – Sep. 8<sup>th</sup>, 2022.

The aerodynamic effects of high-speed trains can cause a number of safety issues, including crosswind effects and high-speed train driving safety, the lift force of the tail vehicle and its operational safety, transient pressure impulses and problems related to strength, structural and operational safety, train-induced winds, and passenger safety on facilities and platforms along the platform.

In strong crosswinds, the aerodynamic coefficient increases rapidly with increasing yaw angle. Increased aerodynamic force (moment) has a significant impact on the lateral stability of high-speed trains and can cause train derailments and overturning.[4]

The streamlined head of a high-speed train can reduce the both the aerodynamic drag and noise. However, a number of vortices are generated behind the streamlined head of the tail vehicle. The vortices behind the tail vehicle can cause a large lift force in the tail vehicle, which will significantly affect the operational safety of the tail vehicle.

#### C. Noise

Noise has become a major challenge and constraint as aerodynamic effects have dominated the dynamic environment of high-speed trains. According to theoretical research and test results on railway noise in China and elsewhere, train noise mainly consists of engine noise, wheel/railway noise, and aerodynamic noise.[4]

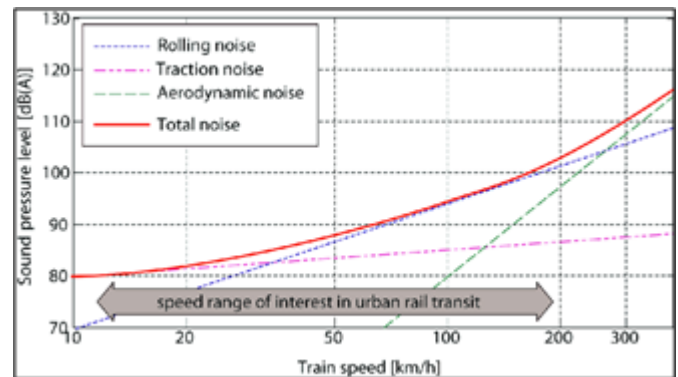


Fig. 3: Train noises and their relationship with train speed.[4]

Studies show that at train speeds of 300 km/h, aerodynamic noise outweighs wheel-rail noise and becomes the main noise of the train. Aerodynamic noise has a great impact on the environment. Excessive environmental noise pollution is an important factor limiting the increase in train speed.

### IV. PRESET CFD STUDY

#### A. Numerical model

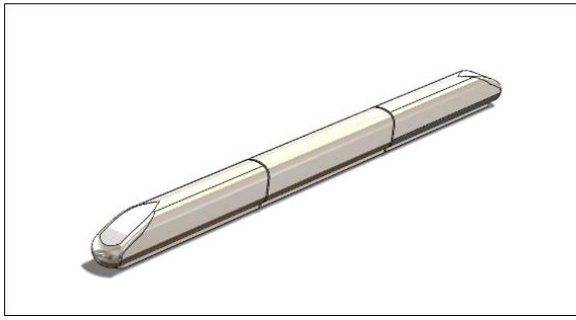


Fig. 4: The model used in the present simulation.

In general, a high-speed train must have at least three vehicles (head car, middle car, and tail car), and was constructed by Solidworks software[5], Fig 4.

### B. Calculation domain and boundary conditions

TABLE I  
Boundary conditions

	ID	B.C
1	wind inlet	velocity inlet
2	wind exit	pressure outlet
3	train body	wall
4	Road	wall
5	domain top surface	symmetry

Computational domain of the present model is shown in Fig.5. All computations were carried out by ANSYS-Fluent software. [6]Table 1 gives the details of the boundary conditions.

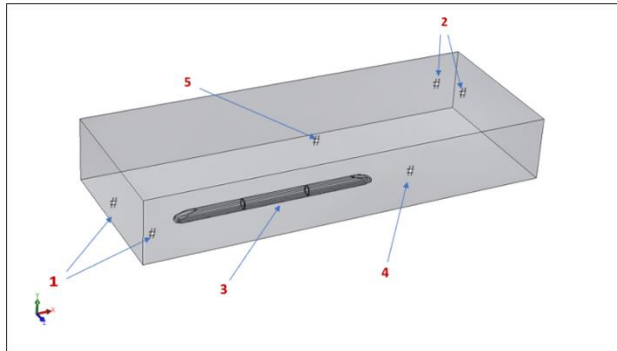


Fig. 5: CFD domain.

### C. Turbulence model

SST K-  $\omega$  Turbulence model was used, which is a two-equation eddy-viscosity model that is used for many aerodynamic applications.[7] It is a hybrid model combining the Wilcox k- $\omega$  and the k- $\epsilon$  models.

### D. Calculation hypothesis

The flow was assumed to be incompressible because Mach number is less than 0.3. Reynolds number is higher than  $10^6$ . So, the flow is turbulent. Train dimensions (head, middle and tail car length equals 25 m, train height and width were set to (3.5 m and 3.3 m, respectively). Some detail structures on vehicle body were ignored to simplify the calculations. Total simulation time was 60 s with 0.01s time-step size.

### E. Computational Mesh

The mesh divisions and quality have a direct impact on computational accuracy and stability. A relatively big mesh size was used for the whole computational domain and small size mesh was used near the train wall with inflation layers, Figs. 6-8.

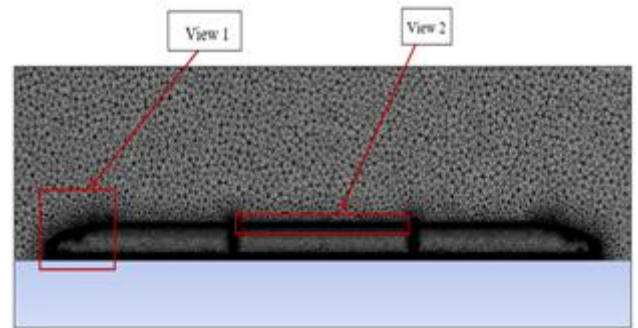


Fig. 6 Mesh overview.[6]

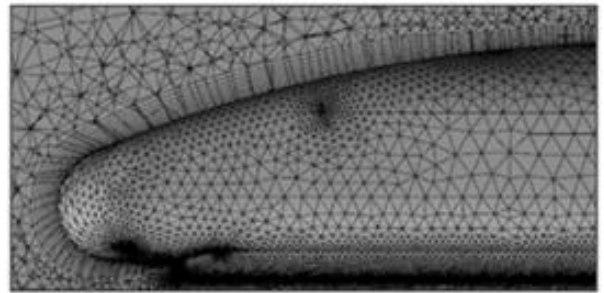


Fig. 7 Inflation layer on the nose of train.[6]

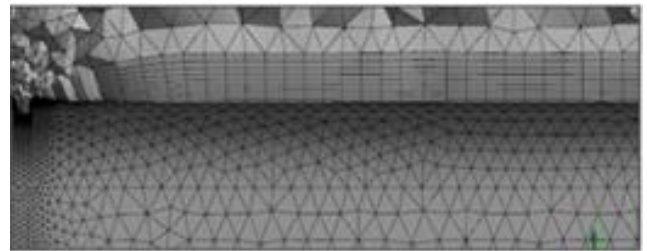


Fig. 8 Inflation layer on the middle car.[6]

Number of elements = 5,635,202

Transition ratio of inflation layer= 0.272.

Number of layers= 10.

#### F. Calculation method

Figure9 shows vector diagram. that relates the wind speed  $u$ , wind angle of attack  $\beta$  and train velocity  $v$ . [8]  
The wind speed relative to the vehicle,  $V$ , is given by:

$$V^2 = (v + u \cos \beta)^2 + (u \sin \beta)^2 \quad (2)$$

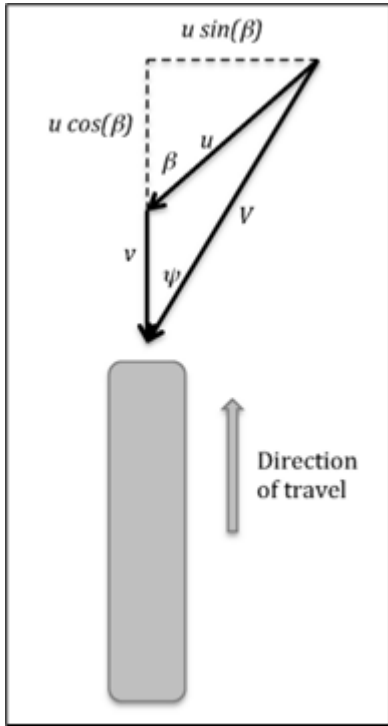


Fig. 9 Velocity vectors.[7]

The wind angle,  $\psi$ , relative to the moving vehicle is given by:

$$\tan \psi = \frac{u \sin \beta}{v + u \cos \beta} \quad (3)$$

#### V. STUDY RESULTS

In order to study aerodynamic forces acting on a high-speed train, computational simulations of two train speeds (100 km/h, 300 km/h) were implemented.

For each speed, four different angles (0,30,60,90) were studied using yaw angle method. For train speed 100Km/h, we will use wind speed was 12 m/s. and for train speed 300 km/h, wind speed was 15 m/s.

##### A. First case

6<sup>th</sup> IUGRC International Undergraduate Research Conference,  
Military Technical College, Cairo, Egypt, Sep. 5<sup>th</sup> – Sep. 8<sup>th</sup>, 2022.

TABLE II  
Forces at different angles of attack, at 100 km/h

Angel of attack	Drag force	Lift force	Side force
$\beta = 0$	2736.1022 N	1509.8867 N	283.03868 N
$\beta = 30$	3280.3621 N	9540.9317 N	-9514.5311 N
$\beta = 60$	2695.9726 N	24134.863 N	-21990.914 N
$\beta = 90$	1432.3459 N	34651.737 N	-25177.475 N

Table 2 shows the value of forces acting on the train.

Turbulent kinetic energy distribution along the train (y-z plane) are shown in Figs. 9-12 for different wind angles, at 100 km/h.

- Wind angle  $\beta=0$

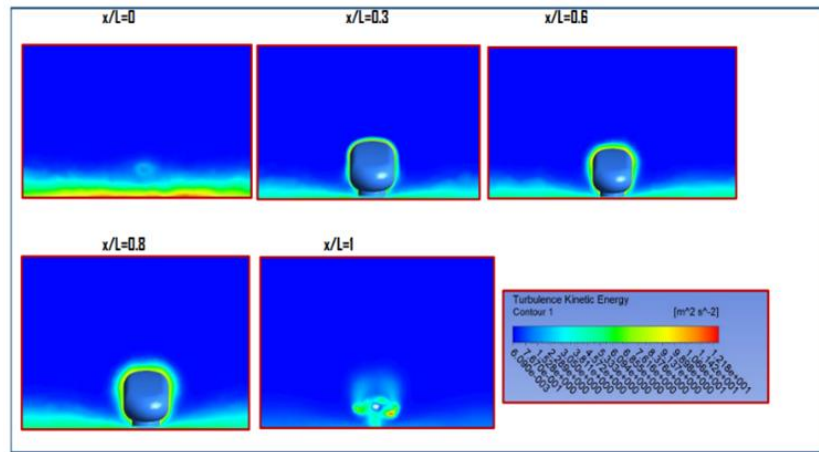


Fig. 9. Turbulent kinetic energy contours, at 100 km/h.

- Wind angle  $\beta=30$

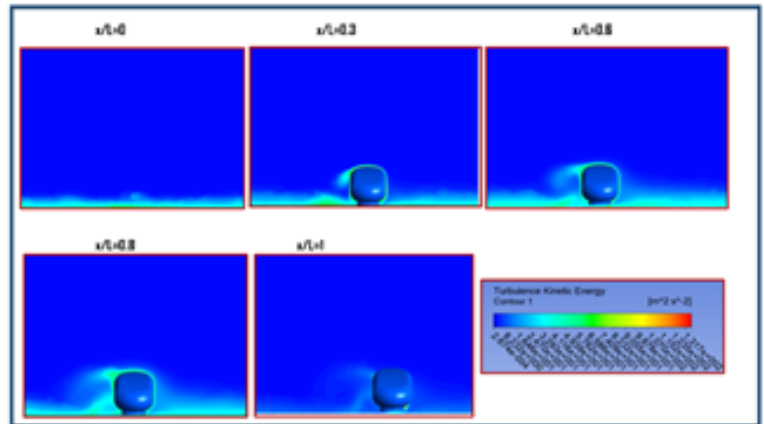


Fig. 10. Turbulent kinetic energy contours, at 100 km/h.

- Wind angle  $\beta=60$

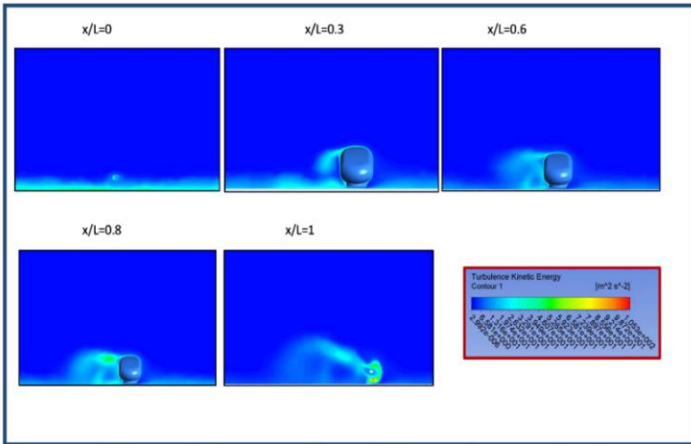


Fig. 11. Turbulent kinetic energy contours, at 100 km/h.

- Wind angle  $\beta=90$

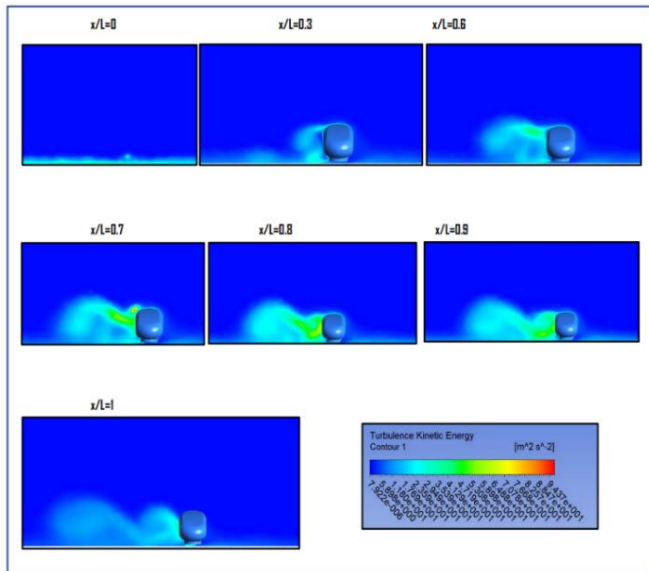


Fig. 12. Turbulent kinetic energy contours, at 100 km/h.

B. Second case

TABLE III  
Forces at different angles of attack, at 300 km/h

Angel of attack	Drag force	Lift force	Side force
$\beta = 0$	17031.737 N	-1410.3697 N	4028.2242 N
$\beta = 30$	17886.782 N	16445.843 N	-20430.412 N
$\beta = 60$	73971.957 N	-17601.18 N	-52645.962 N
$\beta = 90$	14656.318 N	-56607.867 N	-54860.432 N

Table 3 shows the value of the forces acting on the train. Turbulent kinetic energy distribution along the train (y-z plane) are shown in Figs. 13-16 for different wind angles.

- Wind angle  $\beta=0$

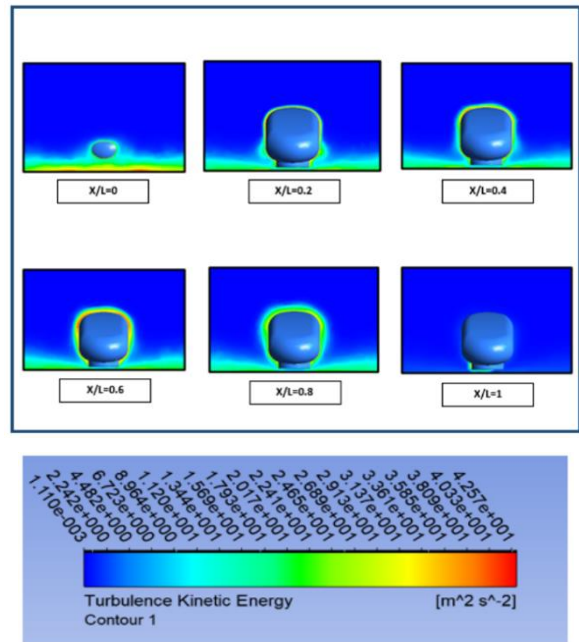


Fig. 13. Turbulent kinetic energy contours, at 300 km/h.

- Wind angle  $\beta=30$

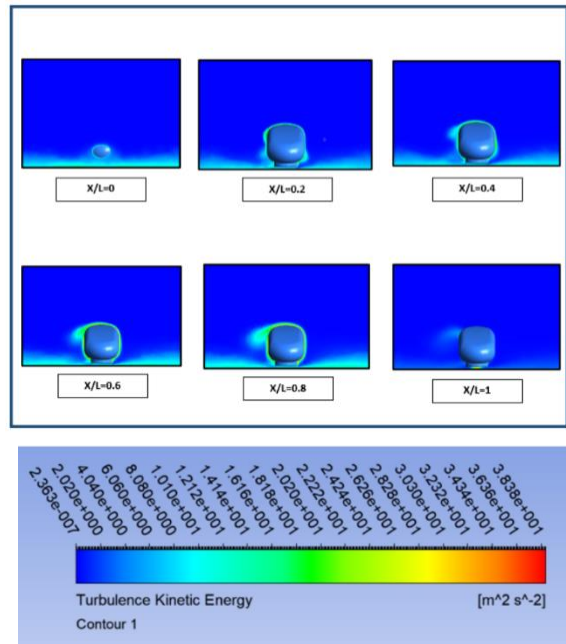


Fig. 14. Turbulent kinetic energy contours, at 300 km/h.

- Wind angle  $\beta=60$

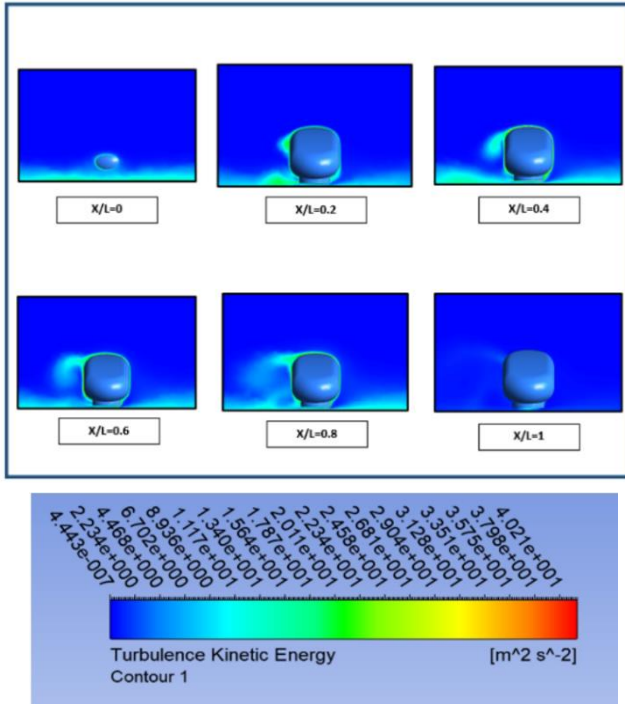


Fig. 15. Turbulent kinetic energy contours, at 300 km/h.

- Wind angle  $\beta=90$

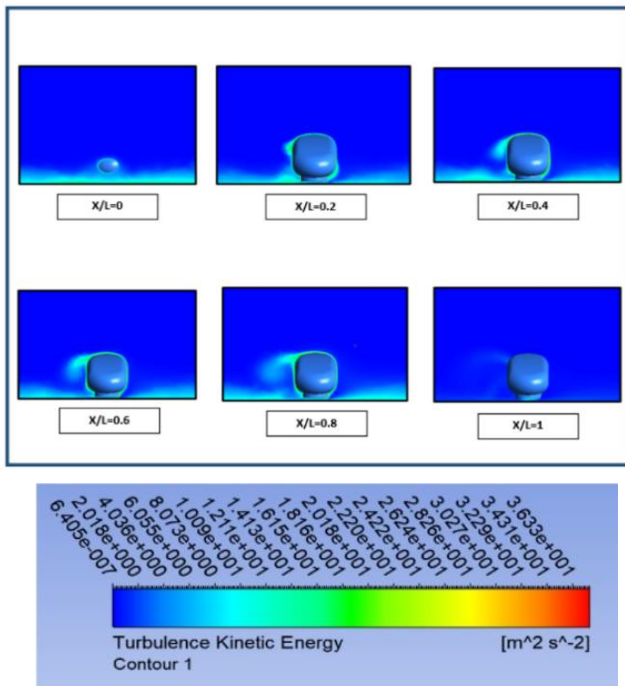


Fig. 16. Turbulent kinetic energy contours, at 300 km/h.

## VI. STABILITY ANALYSIS

The crosswind has a great influence on the dynamic behaviour of a train running on track, especially in high-speed operation. In this section, computational simulation was carried out with the method described before for a high-speed EMU train running on a ballasted track in crosswinds. When a train is running on the track, a priority must be given to the running safety, especially in crosswind environment. There are four indices commonly used as safety criteria in vehicle system dynamics (Garg and Dukkipati 1984)[7], *i.e.*, the derailment coefficient, the wheel-load reduction ratio, the overturning coefficient, and the wheel-rail lateral force.[9]

### A. Derailment coefficient

In the vehicle dynamics, the derailment coefficient is often adopted to estimate the possibility of vehicle derailing. According to the specifications for running safety of railway vehicles used in Chinese Railways, the limit of derailment coefficient is 0.8 for high-speed trains. Fig. 17 compares the maximum derailment coefficients of the three cars at different cross wind speeds, under the train speed of 300 km/h.[9]

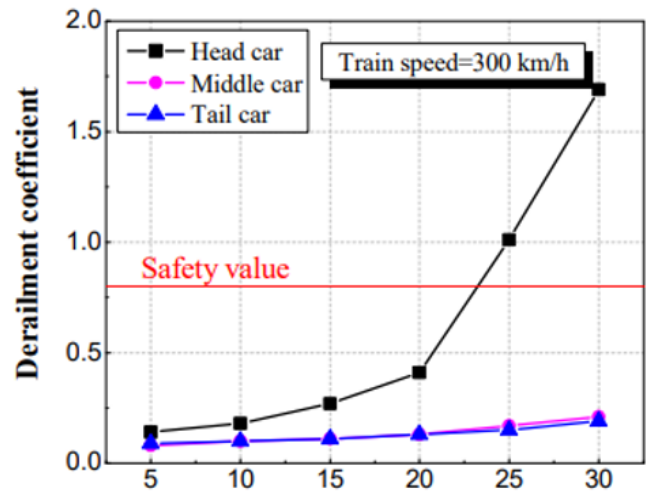


Fig. 17: Derailment coefficient Vs wind speed.

When the wind force is acting on the car body, the dynamic performances of the wheels on the windward side and the leeward side are different. The comparisons of the derailment coefficients between the windward side and the leeward side are carried out in Figs.18(a)-18(b)-18(c) for the head, middle and tail cars, respectively. All the graphs show that the derailment coefficients on the leeward side are larger than those on the windward side in crosswinds. Particularly, for the head car, the difference between the windward side and the leeward side is pronounced at the crosswind speed above 15 m/s.[9]

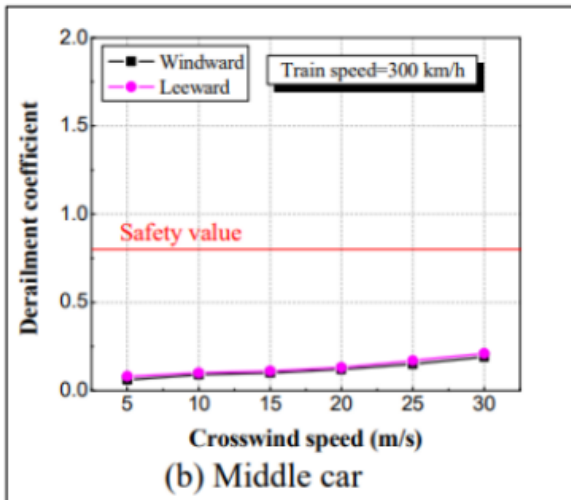
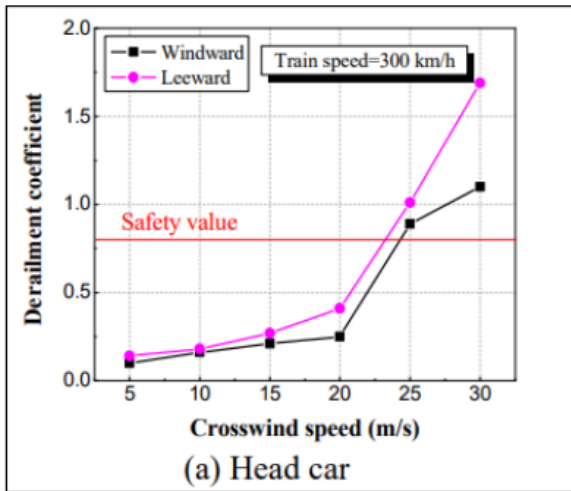
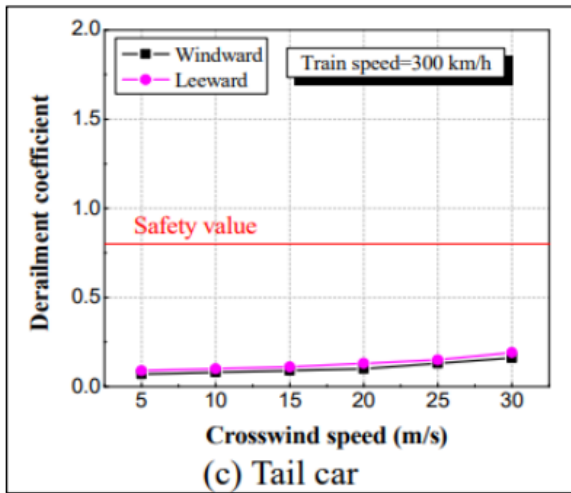


Fig. 18: Deraiment coefficient Vs wind speed on the three different cars.

### B. Wheel-load reduction ratio

The wheel-load reduction ratio is another important index used for estimating the running safety of the train. If the wheel-load of the train is greatly reduced, the operational safety of high-speed train will be seriously threatened. The threshold of dynamical wheel-load reduction ratio is set as 0.9 for some evaluation tests of train dynamic performance in China (Zhai 2015)[9]. the maximum reduction ratios of wheel-load at different crosswind speeds, with the train speed of 300 km/h. are shown in fig.19. It is seen that, with the increase of crosswind speed, the wheel-load reduction ratio rises most quickly for the head car, followed by the middle car, and finally the tail car.

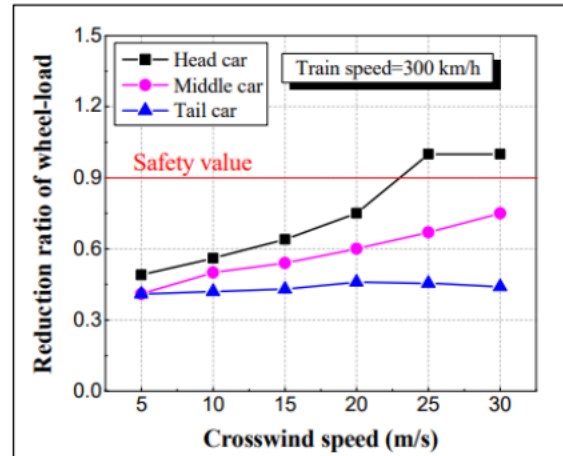


Fig. 19: Wheel-load reduction ratio and wind speed.

### C. Wheel-rail lateral force

In order to prevent the damage of track structure, the wheel-rail lateral force is usually not allowed to exceed 0.4 times of the static axle load. For the train used in this study, the threshold of the wheel-rail lateral force is 53 kN. In Fig.20, the maximum wheel-rail lateral forces on the three cars at different crosswind speeds are compared, with the train speed of 300 km/h. There is no evident discrepancy in all cases at low crosswind speeds. With the increase of the wind speed, the wheel-rail lateral forces in all cases rise more or less, where the growth of the head car is much faster than the other two. For example, when the crosswinds speed reaches 30 m/s, the wheel-rail lateral force of the head car is 158.96 kN.[9]

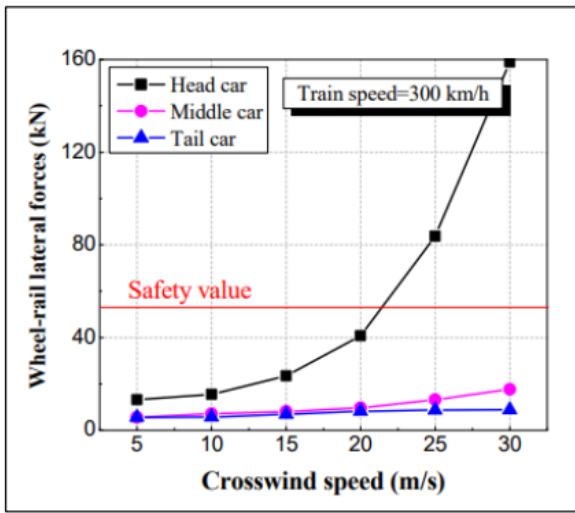


Fig. 20: Wheel-rail lateral forces Vs wind speed.

#### D. Overturning coefficient

Several methods and criteria exist to describe the overturning of a rail vehicle, at steady or unsteady crosswind, and have been used in various studies and in standards. Moment method: the moment method calculates moments about the leeward/outer rail. The method requires the aerodynamic loads on the vehicle and compares the stabilizing moment due to the gravity forces of the vehicle with the overturning moment due to the aerodynamic and centrifugal loads. fig.21 If these moments are equal, the vehicle starts to overturn. When the overturning coefficient is above 0.8, the running train is considered as dangerous in Chinese Railways.[9]

TABLE IV  
Characteristics of the train

Elements	Value
H	3.89 m
W	3.265 m
$B_0$	1.435 m
M	27937.5 Kg

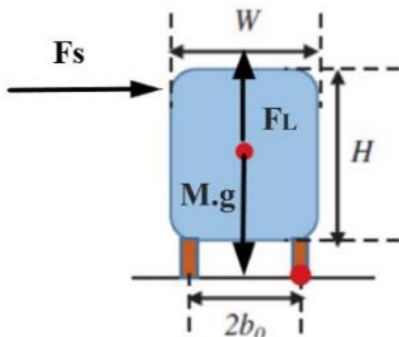


Fig. 21: Forces on train body [2]

Weight of three cars =  $83812.5 \times 9.8 = 821,362.5$  N, so moment due to the weight =  $821,362.5 \times 1.435 = 1,178,655.188$  N.m.

TABLE V

Moments results from the side force

angle $\beta$	0	30	60	90
100 km/h	1101.02	37011.53	85544.66	97940.38
300 km/h	15669.79	79474.3	204792.79	213407.08

#### ROLLING MOMENT

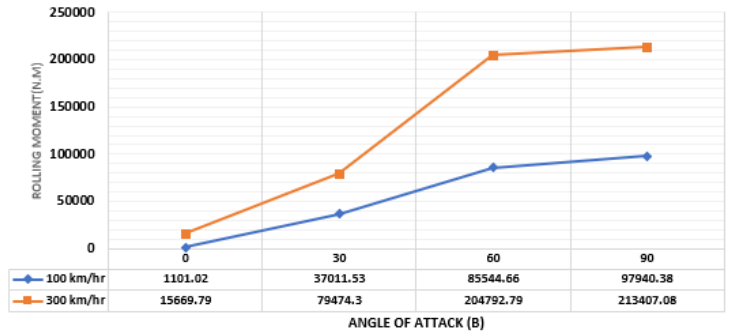


Fig. 22: Rolling moment vs angel of attack

TABLE VI

Moments results from the lift force

angle $\beta$	0	30	60	90
100 km/h	2166.69	13691.24	34633.53	49725.24
300 km/h	2023.88	23599.78	25257.69	81232.29

#### PITCHING MOMENT

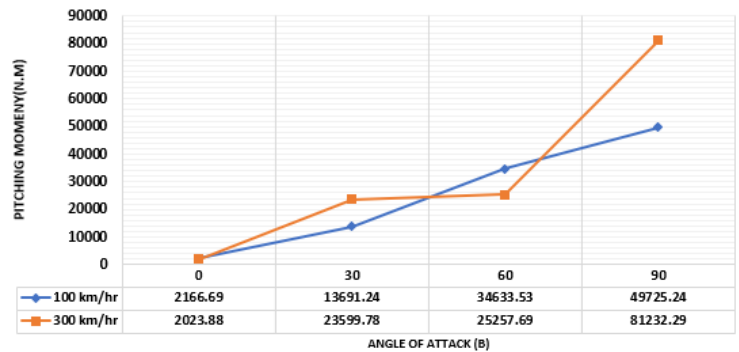


Fig. 23: Pitching moment vs angle of attack



TABLE VII

Moments results from different forces

angle $\beta$	0	30	60	90
100 km/h	3267.71	50702.76	120178.18	147665.62
300 km/h	17693.67	103074.09	230050.49	294639.37

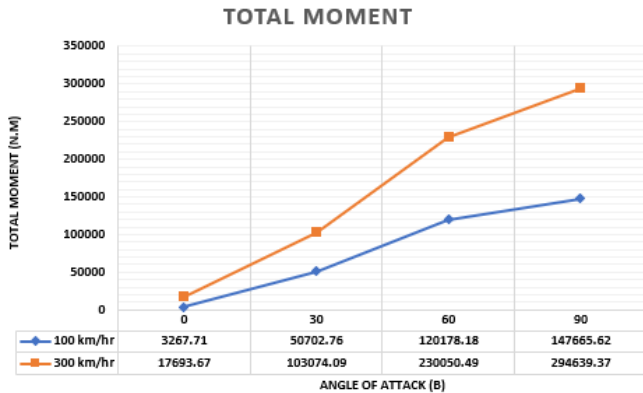


Fig. 24: Total moment vs angle of attack

The moments due to the different forces are shown in table 7. The maximum overturning coefficients at different crosswind speeds and different train speeds are described in Figs 25 and 26.[9]

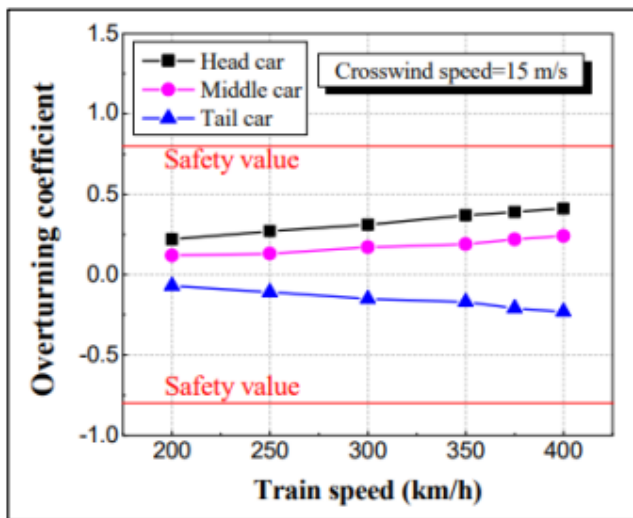


Fig. 25: Overturning coefficient Vs wind speed.

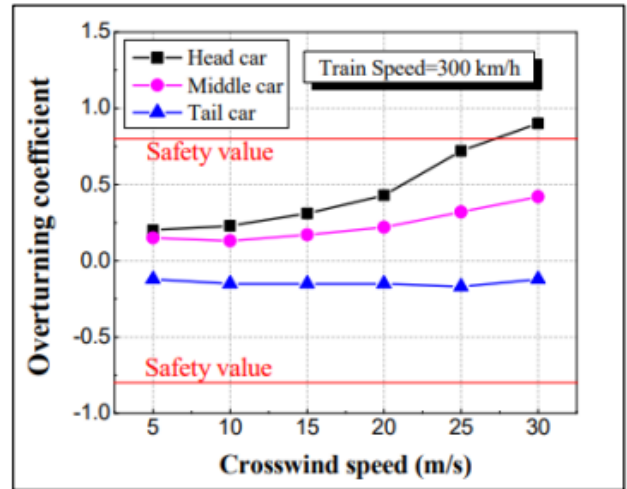


Fig. 26: Overturning coefficient Vs train speed.

## VII. SUGGESTION TO AVOID OVERTURNING

It is suggested to install a sensor to measure crosswind speed, pressure measurement sensor is chosen, which converts an input mechanical pressure of gases or liquids into an electrical output signal, Fig.27.



Fig. 27: Pressure sensor

The movement transducer converts force, pressure, tension, compression, torque, and weight into a change in electrical resistance, which can then be measured. Strain gauges are electrical conductors tightly attached to a film in a zigzag shape. When this film is pulled, it the conductors stretches and elongates. When it is pushed, it is contracted and gets shorter. This change in shape causes the resistance in the electrical conductors to also change. The strain applied in the load cell can be determined based on this principle, as strain gauge resistance increases with applied strain and diminishes with contraction.

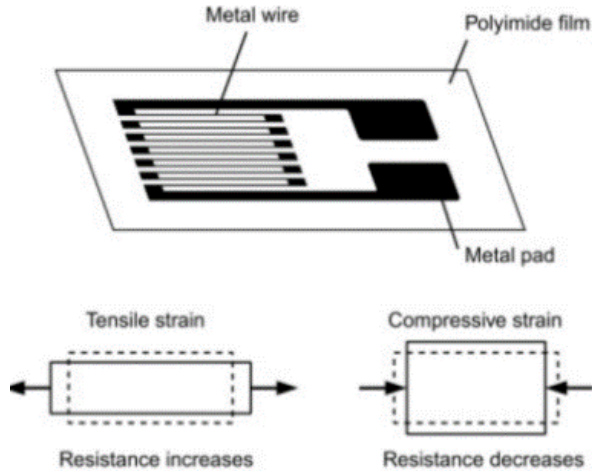


Figure28: Strain gauge

### VIII. MODEL OF TRAIN WITH SENSORS



Fig. 29: Model of train with installed sensors

Fig. 29 shows the train model with the suggested installed sensors.

The idea is that the train speed should be reduced, based on the sensor's readings, when forces/moments read some pre-specified critical values.

### IX. CONCLUSION

For head and tail cars, streamlined areas are most critical for crosswinds. On the windward side, there is a large positive pressure area on the nose of the head car. On the leeward side, almost the entire streamlined area of the head car is a negative pressure area. And the value of negative pressure is very large. The huge difference in pressure between the two sides causes the head car to experience huge side forces. In the tail car, the situation was exactly the opposite. The area and value of

negative pressure on the windward side of the streamlined area of the tail car are larger than those on the leeward side. These results in the streamlined area of the trailing car is mainly subjected to the pull by the crosswinds rather than a thrust.[9]

### X. ACKNOWLEDGMENT

We would like to acknowledge *Prof. Dr. Ahmed Farouk Abdel Gawad, Prof. Dr. Mofreh Melad Nassief Zagazig University* for their support and helping us.

### XI. REFERENCES

- [1] S. S. Ding, Q. Li, A. Q. Tian, J. Du, and J. L. Liu, "Aerodynamic design on high-speed trains," *Acta Mechanica Sinica/Lixue Xuebao*, vol. 32, no. 2, pp. 215–232, Apr. 2016, doi: 10.1007/s10409-015-0546-y.
- [2] I. A. Ishak, M. S. Mat Ali, M. F. Mohd Yakub, and S. A. Z. Shaikh Salim, "Effect of crosswinds on aerodynamic characteristics around a generic train model," *International Journal of Rail Transportation*, vol. 7, no. 1, pp. 23–54, 2019, doi: 10.1080/23248378.2018.1424573.
- [3] A. Dillmann and A. Orellano, "Lecture Notes in Applied and Computational Mechanics 79 The Aerodynamics of Heavy Vehicles III Trucks, Buses and Trains." [Online]. Available: <http://www.springer.com/series/4623>
- [4] L. Zhang, J. ye Zhang, T. Li, and Y. dong Zhang, "Multi-objective aerodynamic optimization design of high-speed train head shape," *Journal of Zhejiang University: Science A*, vol. 18, no. 11, pp. 841–854, Nov. 2017, doi: 10.1631/jzus.A1600764.
- [5] "solidworks, <https://www.solidworks.com/>[Last retrieved: July 2022]," 2016.
- [6] "ANSYS 17.1 <https://www.ansys.com/news-center/press-releases/05-09-16-ansys-171-delivers-optimized-system-performance-for-early-design-process> [Last retrieved: July 2022]," 2016.
- [7] Z. Yao, N. Zhang, X. Chen, C. Zhang, H. Xia, and X. Li, "The effect of moving train on the aerodynamic performances of train-bridge system with a crosswind," *Engineering Applications of Computational Fluid Mechanics*, vol. 14, no. 1, pp. 222–235, 2020, doi: 10.1080/19942060.2019.1704886.
- [8] M. Gallagher *et al.*, "Trains in crosswinds – Comparison of full-scale on-train measurements, physical model tests and CFD calculations," *Journal of Wind Engineering and Industrial Aerodynamics*, vol. 175, pp. 428–444, Apr. 2018, doi: 10.1016/j.jweia.2018.03.002.
- [9] F. Dorigatti, M. Sterling, C. J. Baker, and A. D. Quinn, "Crosswind effects on the stability of a model passenger train-A comparison of static and moving experiments," *Journal of Wind Engineering and Industrial Aerodynamics*, vol. 138, pp. 36–51, 2015, doi: 10.1016/j.jweia.2014.11.009.